RESEARCH ARTICLE

AMERICAN JOURNAL OF medical genetics PART A

IGF1R Variants Associated With Isolated Single Suture Craniosynostosis

Michael L. Cunningham,[1,2,3]* Jeremy A. Horst,[3] Mark J. Rieder,[4] Anne V. Hing,[1,2] Ian B. Stanaway,[4] Sarah S. Park,[1,2] Ram Samudrala,[3,5] and Matthew L. Speltz[1,6]

[1]Seattle Children's Hospital Craniofacial Center, University of Washington, Seattle, Washington 98195

[2]Department of Pediatrics, University of Washington, Seattle, Washington 98195

[3]Department of Oral Biology, University of Washington, Seattle, Washington 98195

[4]Department of Genome Sciences, University of Washington, Seattle, Washington 98195

[5]Department of Microbiology, University of Washington, Seattle, Washington 98195

[6]Department of Psychiatry & Behavioral Sciences, University of Washington, Seattle, Washington 98195

Received 11 August 2010; Accepted 2 October 2010

The genetic contribution to the pathogenesis of isolated single suture craniosynostosis is poorly understood. The role of mutations in genes known to be associated with syndromic synostosis appears to be limited. We present our findings of a candidate gene resequencing approach to identify rare variants associated with the most common forms of isolated craniosynostosis. Resequencing of the coding regions, splice junction sites, and 5′ and 3′ untranslated regions of 27 candidate genes in 186 cases of isolated non-syndromic single suture synostosis revealed three novel and two rare sequence variants (R406H, R595H, N857S, P190S, M446V) in insulin-like growth factor I receptor (*IGF1R*) that are enriched relative to control samples. Mapping the resultant amino acid changes to the modeled homodimer protein structure suggests a structural basis for segregation between these and other disease-associated mutations found in . These data suggest that *IGF1R* mutations may contribute to the risk and in some cases cause single suture craniosynostosis.

Key words: craniosynostosis; IGF1R; non-syndromic; isolated; simple; sagittal; coronal; metopic; resequencing; non-synonymous SNP

How to Cite this Article:
Cunningham ML, Horst JA, Rieder MJ, Hing AV, Stanaway IB, Park SS, Samudrala R, Speltz ML. 2011. *IGF1R* Variants Associated With Isolated Single Suture Craniosynostosis. Am J Med Genet Part A 155:91–97.

INTRODUCTION

The birth prevalence of isolated craniosynostosis is 1/1,700–2,500 live births [Shuper et al., 1985; French et al., 1990], while the prevalence of the syndromic forms (hereditary forms with extracranial malformations) is approximately 1/25,000 [Cohen, 1979; Meyer, 1981]. Mutations in *TWIST1*, *FGFR1*, *FGFR2*, *FGFR3*, *EFNB1*, *TGFBR1*, and *TGFBR2* have been described in cases of single suture craniosynostosis [Passos-Bueno et al., 2008]; however, extracranial manifestations are common and, with the exception of $FGFR3^{P250R}$, isolated single suture craniosynostosis is exceptionally rare in the presence of these mutations. In this study we utilized resequencing to identify rare and private mutations in candidate genes selected on the basis of involvement with syndromic craniosynostosis or cranial suture biology. We report on 3/186 individuals with non-synonymous variants in insulin-like growth factor I receptor (*IGF1R*) that were not observed in 1,000 control genomes (2,000 chromosomes) and two rare *IGF1R* variants that occurred in 0.1–0.3% of controls.

The occurrence of cytogenetic rearrangements in children with craniosynostosis is well described. Among individuals with craniosynostosis and associated malformations and/or developmental delay, approximately 10–16% will have detectable chromosome abnormalities [Cohen and MacLean, 2000; Passos-Bueno et al., 2008]. Even though rare cytogenetic rearrangements may not account for a large number of affected individuals, detection of such events can point to mutations that cause human malformation. Through a detailed review of the literature, we have catalogued

Grant sponsor: NIH grants; Grant numbers: NIH/NIDCR R01 DE018227, NIH/NIDCR R01 DE013813 NIH/NIDCR F30 DE017522; Grant sponsor: Jean Renny Endowment for Craniofacial Research.

*Correspondence to:
Michael L. Cunningham, MD, PhD, Department of Pediatrics, University of Washington, Seattle, WA 98195, USA. Seattle Children's Hospital, 4800 Sand Point Way NE, MS W7847, USA. E-mail: mcunning@uw.edu

Published online 22 December 2010 in Wiley Online Library (wileyonlinelibrary.com).
DOI 10.1002/ajmg.a.33781

13 chromosomal aberrations for which two or more individuals with craniosynostosis have been reported. In addition to regions known to harbor known craniosynostosis genes 5q35 duplication (*MSX2*) and 7p21 deletion (*TWIST1*) [Ma et al., 1996; Sood et al., 1996; Howard et al., 1997], we found five additional chromosomal regions containing genes involved in calvarial development including *TGFB2* (1q41), *FGF2* (4q26), *IGF2R* (6q26), *IGFBP1/IGFBP3* (7p14), and notably for this study, *IGF1R* (15q25-qter) [Gabbitas and Canalis, 1998; Cano-Gauci et al., 1999; Adab et al., 2002; Ben Lagha et al., 2006; Fulzele et al., 2007].

In total, there have been six case reports of trisomy (or tetrasomy) of chromosome 15q25-qter (inclusive of the *IGF1R* locus) in individuals with craniosynostosis (sagittal, metopic, and multi-suture synostosis), indicating a potential role for dosage of *IGF1R* in premature suture fusion [Pedersen, 1976; Van Allen et al., 1992; Van den Enden et al., 1996; Zollino et al., 1999; Hu et al., 2002; Nagai et al., 2002]. Additionally, postnatal overgrowth has been reported in individuals with extra copies of the *IGF1R* gene [Kant et al., 2007], whereas growth retardation is noted in those with monosomy 15q26 (*IGF1R*) [Veenma et al., 2010], suggesting a dosage effect of a growth stimulatory gene.

IGF1R, located at 15q26.3, is a tyrosine kinase growth factor receptor with significant homology to the insulin receptor (INSR) and serves as the receptor for both IGF-I and IGF-II. IGF-I and IGF1R are both expressed in the developing cranial sutures, where they regulate bone growth and increase expression in response to tensile force [Roth et al., 1997; Bradley et al., 1999; Hirukawa et al., 2005]. In a mouse explant suture model, exogenous IGF-I has been shown to induce increased expression of osteocalcin, osteopontin, alkaline phosphatase, and type 1 collagen [Chen et al., 2003]. Furthermore, increased systemic thyroxine exposure, a known cause of craniosynostosis in humans, leads to increased IGF-I expression in the sagittal suture [Akita et al., 1996]. An interaction between IGF1R and fibronectin has been shown to inhibit apoptosis in pancreatic carcinoma cell lines through IGF1R transactivation [Edderkaoui et al., 2007]. The occurrence of overgrowth and craniosynostosis in humans with *IGF1R* trisomy/tetrasomy, its proliferative and anti-apoptotic activities, and its role in bone growth suggests that gain-of-function mutations in *IFG1R* could lead to craniosynostosis.

In this manuscript we describe five individuals with isolated single suture craniosynostosis associated with either private or exceptionally rare variants of *IGF1R*. We suggest that individuals with mutations in *IGF1R* have an increased risk of developing craniosynostosis.

MATERIALS AND METHODS

Participants and DNA Sample Preparation

We obtained independent prospective institutional review board (IRB) approval from each participating center: including Seattle Children's Hospital, Northwestern University in Chicago, Children's Heath Care of Atlanta, and St. Louis Children's Hospital. This study is HIPAA compliant.

Participants were enrolled in a previously described, prospective, four-center investigation of neurodevelopment among children with single suture craniosynostosis [Speltz et al., 2007]. Infants were eligible if, at the time of enrollment, they had isolated sagittal, unilateral coronal, metopic, or unilateral lambdoid synostosis confirmed by CT scan. Lambdoid synostosis cases were excluded from the present study due to insufficient numbers. Exclusion criteria included presence of major medical or neurological conditions; presence of three or more minor extra-cranial malformations [Leppig et al., 1987]; or presence of other major malformations.

Enrolled cases in the overall study were 84% of those eligible, with distance or time constraints being the major reason for non-participation. CT scans were performed at each participating center and used for diagnosis confirmation. Neurodevelopmental data were available for 136 cases enrolled in the present study. We administered two standardized, norm-referenced tests at age 3, the Bayley Scales of Infant Development—2nd Edition (BSID-II) [Black and Matula, 1999] and the Preschool Language Scale, Third Edition (PLS-3) [Zimmerman et al., 1991]. DNA was isolated with routine methods. Prior to enrollment in this study all cases were screened for hotspot mutations in *FGFR1*, *FGFR2*, *FGFR3*, *TWIST1*, and *MSX2* [Seto et al., 2007], and all females for mutations in *EFNB1* (data not shown) and excluded from this study if a causative mutation was identified. Each of these genes was resequenced in enrolled cases to identify novel variants outside of mutation hotspot regions.

Resequencing

DNA from 186 craniosynostosis cases (46 coronal, 46 metopic, and 94 sagittal) and 95 screening control genomes (Coriell, Camden, NJ) drawn from major US populations (African/African–American, European, Asian {Chinese/Japanese}, and Hispanic), used previously as part of the NIEHS-SNPs Environmental Genome Project, were used for candidate gene resequencing. Twenty-seven candidate genes chosen on the basis of involvement with syndromic craniosynostosis and/or suture development (*EFNB1*, *FGFR1*, *FGFR2*, *FGFR3*, *MSX2*, *NELL1*, *TWIST1*, *EFNA4*, *FGF2*, *RUNX2*, *SNAI1*, *TWIST2*, *TGFβR1*, *TGFβR2*, *ALX4*, *BMP2*, *BMP3*, *BMP4*, *BMP7*, *IFG1R*, *IGF-I*, *IGF2R*, *IGFBP1*, *IGFBP5*, *TGFβ1*, *TGFβ2*, and *TGFβ3*) were sequenced in all coding regions, splice junction sites, and 5′ and 3′ untranslated regions.

Control Genotyping

Genetic variants identified in the candidate genes of cases, but not the 95 Coriell controls, were subjected to site-specific genotyping in a sample of 1,012 control samples sourced from 480 Sigma Human Random Control DNA samples (HRC-1 thru HRC-5, Sigma, St. Louis, MO), 421 de-identified clinical samples from Seattle Children's Hospital, 92 Coriell samples (unique from the screening controls), and 19 samples from subjects with Mendelian disorders with a previously identified molecular cause. The identification of five rare variants in the coding region of *IGF1R* led to further analysis of conservation at the nucleotide and amino acid level as well as protein modeling.

Amino Acid Conservation and GERP Scores

Each variant of interest identified in *IGF1R* was analyzed for evolutionary conservation using the NCBI Multiple Alignment

Viewer within Blink [http://www.ncbi.nlm.nih.gov]. Greater evolutionary conservation was used to prioritize variants for further investigation. In addition to measures of evolutionary conservation at the amino acid level, GERP (Genomic Evolutionary Rate Profiling) scores were used as an alternative prioritization tool [Goode et al., 2010]. The GERP score estimates the difference between observed rates of evolution at a given site at the nucleotide level and that expected assuming neutral evolution. A score greater that 4 has been shown to enrich for mutations that cause Mendelian disease [Cooper et al., 2010].

Protein Conformation—Modeling the IGF1R–IGF-I Hetero Quaternary Structure

We built a comprehensive INSR oligomer using the repeating crystal unit cell contacts from the most recent and representative extracellular structure (PDB identifier 2dtg) [Berman et al., 2000]. We identified the dimers spanning the unit cell border as physiologic by evaluating monomer to monomer crystalization artifacts and mapping known mutations associated with insulin resistance. The selected chains are the same as those resulting from previous informatic analysis [Renteria et al., 2008]. Using this structure as a template, we substituted in the available portion of the IGF1R structure (residues E31–E489; PDB identifier 1igr) [Garrett et al., 1998]. We converted the remaining globular extracellular portion of the INSR to represent IGF1R by mutating side chains with SCWRL4 [Krivov et al., 2009]. We rebuilt missing loops with both loop building options in the RAMP (Rapid AutoModelling of Proteins) suite: phi/psi search and segment matching, [http://software.compbio.washington.edu/ramp/ramp.html] and selected loops using Bayesian analysis of inter residue contacts [Samudrala and Moult, 1998]. We docked the IGF-I ligand into the resulting IGF1R homodimer model in the conformation proposed by Epa and Ward (2006). Finally, we rotated domain 3 (L2) around the ligand from the conformation in the 1igr structure to that of insulin in the 2dtg structure, as suggested in the 1igr structure paper [Garrett et al., 1998]. The resulting modeled homodimer presents a cavity with matching topology to IGF-I, and so we present this as the most representative model to date for the IGF1R–IGF-I hetero quaternary structure. Upon this model we mapped all mutations published for IGF1R (selected data shown) and those novel mutations reported here.

RESULTS

Resequencing 27 candidate genes in 186 cases yielded 1,383 polymorphisms. Forty-nine of these polymorphisms were confined to cases (e.g., not seen in screening 95 Coriell genomes). Genotyping of these 49 SNPs in 1,012 control genomes resulted in the identification of 15 private variants in 14 cases (one each in *BMP3*, *BMP4*, *EFNB1*, *FGF2*, *NELL1*, *TGFB3*, two each in *IGF2R*, *TGFBR2*, and *TGFB2*). Five variants were identified in *IGF1R* (Table I), with three being exclusive to a case subject and two found to be exceptionally rare (control minor allele frequency: 0.0005 and 0.0032). None of these five cases had private or rare variants identified in other candidate genes.

Mapping IGF1R Mutations onto the IGF1R/IGF-I Hetero Quaternary Structure

We used the known crystalline structures of IGF1R, INSR, and IGF-I to interpret the location and potential functional significance of the amino acid variants identified in our cohort. Using this method we have determined that all three private variants (R406H, R595H, and N857S) occur in amino acid residues that are located on the external surface of the IGF1R quaternary structure (Fig. 1). In the presented dimeric orientation and all those previously proposed, the mutated residues are exposed with respect to the homodimer partner, the IGF-I binding site, and the cell membrane.

The R406H (domain 3, L2, receptor L-domain) and R595H (domain 4, FN III-0, fibronectin 3 domain) mutations are co-located on the protein surface despite the long intervening sequence of 189 amino acids (Fig. 1). The intervening surface forms a

TABLE I. Novel and Rare IGF1R Variants Associated With Isolated Craniosynostosis

Case	Suture	Domain	Variant	MAF cases (n)	MAF controls (n)	SNP	Conservation	GERP
Private variants								
1	Sagittal	Recep L domain	IGF1R-ARG-0406-HIS	0.003 (1/186)	0.000 (0/916)	0	Fish	5.4
2	Coronal	—	IGF1R-ARG-0595-HIS	0.003 (1/186)	0.000 (0/852)	rs56248469	Mouse, marsupial	4.6
3	Sagittal	FN3 domain	IGF1R-ASN-0857-SER	0.003 (1/186)	0.000 (0/930)	rs45611935	Fish	5.5
Rare variants								
4	Coronal	Furin-like cysteine rich region	IGF1R-PRO-0190-SER	0.003 (1/186)	0.0005 (1/936)	0	Mouse	4
5	Coronal	Recep_L_domain	IGF1R-MET-0446-VAL	0.003 (1/186)	0.0032(6/931)	0	Mouse	5.4

R406H (case 1), R595H (case 2), and N857S (case 3) variants were identified in cases but not in 916, 852, and 930 genomes, respectively. The father of case 1 was found to carry the R406H variant and the mother of case 2 was found to carry the N857S variant. Neither family member was examined but were not reported to have evidence of synostosis. The variants in cases 2 and 3 were each identified in dbSNP (rs56248469 and rs45611935, respectively). In both cases dbSNP recorded a single occurrence in a cancer registry and in neither phenotype nor sample size was reported. Subsequent to enrollment case 5 was found to have stridor, a pituitary cyst, and developmental delays. In all cases the amino acid residues and nucleic acid sequence (GERP score) [Goode et al., 2010] suggested a high level of conservation (GERP score above our threshold of 4 in all five cases). Rare variants P190S (case 4) and M446V (case 5) were seen in the control sample with minor allele frequencies of 0.0005 and 0.0032, respectively. Of note, there are 240 arginine to histidine mutations in the 7,022 disease associated nsSNPs listed in OMIM, such that mutations seen in cases 1 and 2 are enriched 13 fold for disease phenotypes with respect to random [Online Mendelian Inheritance in Man, 2010].
MAF, minor allele frequency; SNP, data from SNP database.

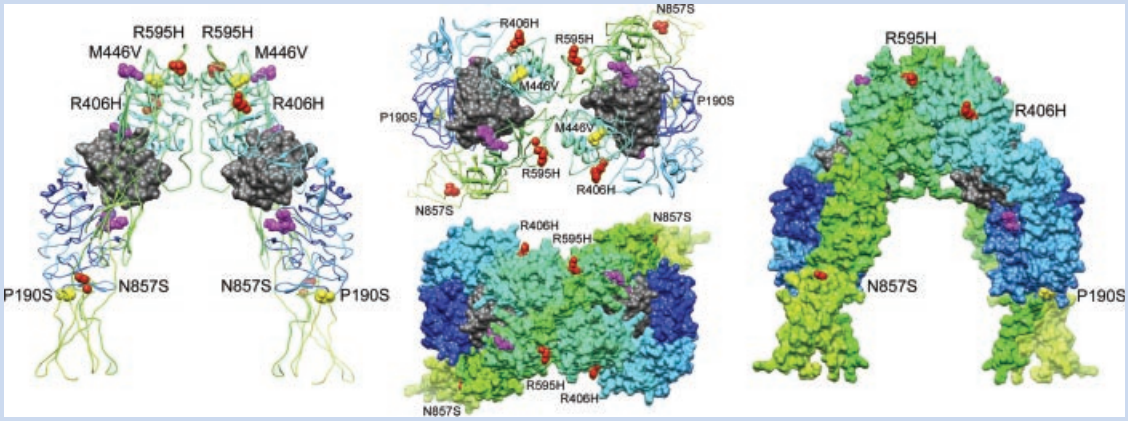

FIG. 1. Structural basis for segregation between disease-associated mutations found in IGF1R. Two IGF1R monomers are each shown with rainbow coloring from amino terminus in blue to carboxy terminus in red (left panel). Only the extracellular domains are represented here. Mapping the novel (red side chains) and rare (yellow side chains) IGF1R missense mutations reveals segregation with respect to mutations associated with growth deficiency (purple side chains), which occur principally at the ligand binding site for IGF-I (gray). Middle panels are oriented with a view from the extracellular space toward the cell membrane; the R406H and R595H mutations both occur within a large elongated concavity (see red side chains in lower middle panel) exhibiting contours and hydrophobicity suggestive of a protein interaction site (see Fig. 2). Surface models (right and lower middle) demonstrate that each novel mutation (R406H, R595H, and N857S) are on the protein surface. M446V is in close proximity with R406H and R595H. In the left panel the N857S and P190S mutations are seen to co-localize at the terminal extent of overlap for the dimer interface.

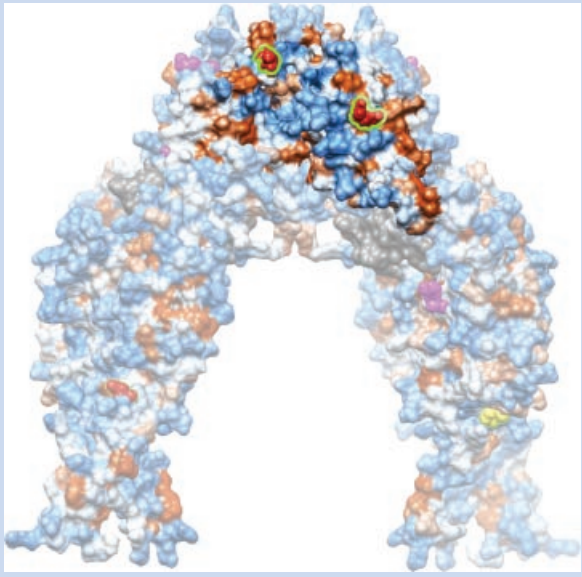

FIG. 2. R595H and R406H map to rim of IGF1R hydrophobic concavity. The R595H and R406H variants (shown with red side chains outlined in green) present in a hydrophobic concavity suggestive of a non-obligate protein interaction. The IGFI–IGF1R heterooligomer surface is shown colored by hydropathicity: hydrophobic surface patches shown as orange, neutral as white, hydrophilicity as blue. A series of hydrophobic patches form the rim of a concavity approximately 15 Å in depth and 30 Å at maximum width. The remaining protein surface is fogged to highlight the concavity, and show the relatively sparse hydrophobicity on the remaining IGF1R surface. Both R595H and R406H private variants map to the rim of this concavity, possibly providing interactions essential to a protein interaction relevant to IGF1R signaling. Orientation: the cell membrane would be at the bottom of image.

concavity (Fig. 1), which collects relatively large patches of hydrophobicity (Fig. 2).

The N857S variant presents in domain 6 on the side opposite the homodimer interface, at the corner of the lateral surface of the construct. There are no previous reports of mutations in IGF1R or the INSR in the immediate area (Figs. 1–3). The rare variants identified in our study (P190S and M446V) demonstrate a high level of conservation at the amino acid and nucleotide (GERP score) level. P190S presents at a similar distance from the cell membrane, similarly exposed at the opposite side of the construct stalk to the private variant N857S (Fig. 1). M446V is in close proximity to the private variants R406H and R595H. Clustering of these private and rare variants identified in cases of craniosynostosis suggests a functional relationship.

Neurodevelopmental Features of Cases With IGF1R Variants

We compared the average BSID-II and PLS-3 standard scores for the five cases with identified rare *IGF1R* variants with the average standard scores of all other enrolled cases for whom we had test data ($n = 136$). As the *IGF1R* variant case sample was too small for meaningful interpretation of inferential statistics, we calculated only means, standard deviations, and effect sizes [Cohen, 1992], which are shown in Table II. At age 3, the mean BSID-II and PLS-3 scores of cases with rare *IGF1R* variants were approximately 2/3 of a standard deviation lower than the mean scores generated by other cases of synostosis for whom we had psychometric test data. However, there was substantial variation in test scores among these five cases with *IGF-1R* variants and the possibility of association between this mutation and neurodevelopmental status requires confirmation in larger samples.

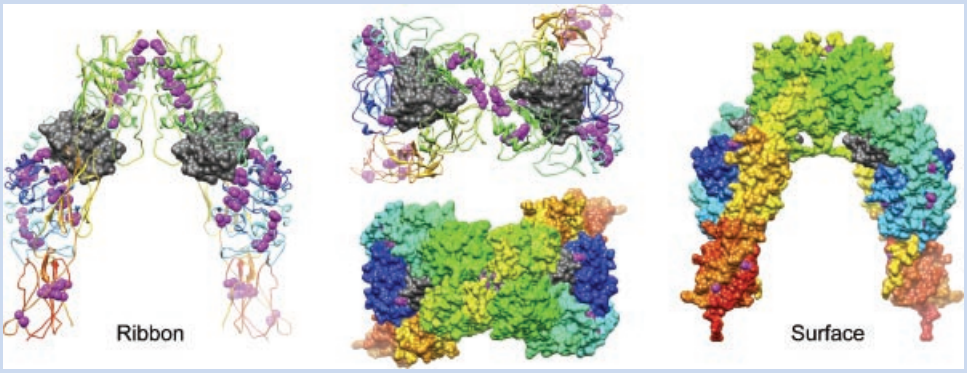

FIG. 3. INSR missense mutations associated with insulin resistance or leprechaunism. Depiction of the INSR dimer and insulin ligand is analogous to those of IGF1R and IGF-I in Figure 1, respectively. The INSR is shown with rainbow coloring from amino terminus in blue to carboxy terminus in red. The insulin ligands are shown in gray. Side chains of previously described missense mutation sites are shown in purple. The mutation sites cluster, in a pattern describing deleterious effects on receptor folding or ligand binding. The IGF1R mutations described in this manuscript are at unique sites with respect to those previously described for the INSR.

DISCUSSION

We report on three cases of isolated sagittal or coronal craniosynostosis with private mutations in *IGF1R* that occur in highly conserved residues on the surface of the functional IGF-I–IGF1R quaternary structure, opposite to the IGF1R homodimer interface, and far from the binding cavity of IGF-I. Previous to this study, no mutations have been described that map to the IGF1R or INSR surface at these variant sites. Previously reported mutations in the extracellular portion of IGF1R are associated with growth retardation, and are primarily confined to the IGF-I interface (Fig. 1, shown in purple). Although postnatal growth information for our cases is not available, trisomy and tetrasomy including 15q26.3 (the chromosomal location of *IGF1R*) is associated with overgrowth and craniosynostosis [Pedersen, 1976; Van Allen et al., 1992; Van den Enden et al., 1996; Zollino et al., 1999; Hu et al., 2002; Nagai et al., 2002; Kant et al., 2007], suggesting an IGF1R gain of function phenotype.

The R406H and R595H residues are separated far in sequence space but physically close even for neighboring domains (23 Å between α-carbons; the diameter of the homodimer construct is 130–150 Å). These residues likely function in the same protein interaction, as they span a hydrophobic surface patch postulated to contribute to protein interaction specificity (Fig. 2) [Garrett et al., 1998]. This hydrophobic surface may interact with a large multidomain protein such as fibronectin, or a subsidiary partner thereof. Enhanced interaction with fibronectin could increase its proposed prosurvival effect [Edderkaoui et al., 2007], thereby increasing the IGF1R signal as a gain of function mutation. Furthermore, the rare variant M446V is in close physical proximity to these private variants. We hypothesize that this protein-binding event is integral to maintaining suture patency during calvarial development.

Previously described missense mutations in the extracellular domains of IGF1R are all associated with growth retardation [Abuzzahab et al., 2003] and are presumed to lead to loss of IGF1R function. The V599E mutation is thought to result in abnormal protein trafficking [Wallborn et al., 2010], the R511Q mutation decreases intracellular signaling response to IGF-1 [Inagaki et al., 2007], the G1125A (a kinase domain mutation) results in a dominant-negative effect [Kruis et al., 2010], and a homozygous non-sense mutation C821Term [Jospe et al., 1996] and a 95 kb deletion of exons 11–21 of *IGF1R* [Veenma et al., 2010] have each been associated with short stature or multiple anomalies associated with growth deficiency. Each of the mutations associated with

TABLE II. Neurodevelopmental Test Scores for Subjects With IGF1R Variants

	Cases with IGF1R variants (n = 5)		Cases without IGF1R variants (n = 131)		
Neurodevelopmental Test (at age 3)	**Mean**	**SD**	**Mean**	**SD**	**Effect Size (d)**
BSID-II MDI	79.4	23.3	93.5	12.9	0.75
BSID-II PDI	81.8	17.3	91.6	13.6	0.63
PLS-3	84.2	17.8	96.9	14.3	0.78

MDI, mental development index; PDI, psychomotor development index; Mean, Standard, norm-referenced scores with a population mean of 100, SD = 15. d, difference between the two means divided by the pooled standard deviation in this sample.

growth deficiency occur in either the ligand binding site or lead to receptor loss of function. The one extracellular *IGF1R* missense mutation associated with growth retardation not shown (R709Q; template not available for the 675–774 region) is spanned closely by positions that significantly decrease or abrogate IGF-I affinity when mutated to alanine [Mynarcik et al., 1997; Whittaker et al., 2001]. In contrast, the three novel mutations and two rare variants we describe herein present in a consistent spatial distribution different from those previously seen for the disease phenotypes of IGF1R (Fig. 1) or INSR missense mutations (Fig. 3).

While also residing on the surface of the extracellular domain of IGF1R, the N857S mutation is not in the same domain as the other two mutations. This variant presents in a cleft not present in the INSR, between a positively charged region of domain 5 and a negatively charged region of domain 6. This interdomain cleft is opposite the terminal extent of the homodimer interface, at which resides the P190S variant site. The proximity of the N857S and P190S variants to the homodimer interface endpoint may describe increased autodimerization, a second postulated mechanism for overgrowth by upregulating IGF1R signaling.

In summary, we have identified private mutations of *IGF1R* in three cases of isolated sagittal or coronal craniosynostosis (R406H, R595H, and N857S). Each of these mutations occurred in residues on the surface of the extracellular domains distant from the IGF binding domain. The rarity of these mutations (<1/2,000 chromosomes), their location in probable protein-binding sites, their co-location with rare variants associated with craniosynostosis (P190S and M446V), and the role of IGF1R in the development of cranial sutures and regulation of osteoblast proliferation suggest that these, and potentially other mutations in *IGF1R*, play a role in the pathogenesis of craniosynostosis. In addition, we have tentatively identified among cases with single-suture craniosynostosis an association between *IGF1R* mutations and elevated risk of neurodevelopmental delay. Future studies of patients with *IGF1R* -associated craniosynostosis will help to elucidate the clinical significance of these mutations. Our ongoing investigation will include in vitro functional analysis and replication of these data in another large craniosynostosis cohort.

ACKNOWLEDGMENTS

This work was supported by NIH grants NIH/NIDCR R01 DE018227 (MLC), NIH/NIDCR R01 DE013813 (MLS), NIH/NIDCR F30 DE017522 (JAH) and the Jean Renny Endowment for Craniofacial Research (MLC). We wish to thank Linda Peters for her assistance in the collection of samples used to for DNA isolation and Jerrie Bishop for her assistance in manuscript preparation.

REFERENCES

Abuzzahab MJ, Schneider A, Goddard A, Grigorescu F, Lautier C, Keller E, Kiess W, Klammt J, Kratzsch J, Osgood D, Pfaffle R, Raile K, Seidel B, Smith RJ, Chernausek SD. 2003. IGF-I receptor mutations resulting in intrauterine and postnatal growth retardation. N Engl J Med 349: 2211–2222.

Adab K, Sayne JR, Carlson DS, Opperman LA. 2002. Tgf-beta1, Tgf-beta2, Tgf-beta3 and Msx2 expression is elevated during frontonasal suture morphogenesis and during active postnatal facial growth. Orthod Craniofac Res 5:227–237.

Akita S, Hirano A, Fujii T. 1996. Identification of IGF-I in the calvarial suture of young rats: Histochemical analysis of the cranial sagittal sutures in a hyperthyroid rat model. Plast Reconstr Surg 97:1–12.

Ben Lagha N, Seurin D, Le Bouc Y, Binoux M, Berdal A, Menuelle P, Babajko S. 2006. Insulin-like growth factor binding protein (IGFBP-1) involvement in intrauterine growth retardation: Study on IGFBP-1 overexpressing transgenic mice. Endocrinology 147:4730–4737.

Berman HM, Westbrook J, Feng Z, Gilliland G, Bhat TN, Weissig H, Shindyalov IN, Bourne PE. 2000. The Protein Data Bank. Nucleic Acids Res 28:235–242.

Black M, Matula K. 1999. Essentials of Bayley Scales of Infant Development II Assessment. New York: John Wiley.

Bradley JP, Han VK, Roth DA, Levine JP, McCarthy JG, Longaker MT. 1999. Increased IGF-I and IGF-II mRNA and IGF-I peptide in fusing rat cranial sutures suggest evidence for a paracrine role of insulin-like growth factors in suture fusion. Plast Reconstr Surg 104:129–138.

Cano-Gauci DF, Song HH, Yang H, McKerlie C, Choo B, Shi W, Pullano R, Piscione TD, Grisaru S, Soon S, Sedlackova L, Tanswell AK, Mak TW, Yeger H, Lockwood GA, Rosenblum ND, Filmus J. 1999. Glypican-3-deficient mice exhibit developmental overgrowth and some of the abnormalities typical of Simpson–Golabi–Behmel syndrome. J Cell Biol 146:255–264.

Chen Y, Zhang DS, Tao PY, Xu P, Feng SZ, Mu XZ, Wei M. 2003. The effect of insulin-like growth factor 1 on the fusion of cranial suture. Zhonghua Zheng Xing Wai Ke Za Zhi 19:11–14.

Cohen MM Jr. 1979. Craniosynostosis and syndromes with craniosynostosis: Incidence, genetics, penetrance, variability, and new syndrome updating. Birth Defects Orig Artic Ser 15:13–63.

Cohen J. 1992. A power primer. Psychol Bull 112:155–159.

Cohen MM, MacLean RE. 2000. Craniosynostosis: Diagnosis, Evaluation, and Management. New York: Oxford University Press.

Cooper GM, Goode DL, Ng SB, Sidow A, Bamshad MJ, Shendure J, Nickerson DA. 2010. Single-nucleotide evolutionary constraint scores highlight disease-causing mutations. Nat Methods 7:250–251.

Edderkaoui M, Hong P, Lee JK, Pandol SJ, Gukovskaya AS. 2007. Insulin-like growth factor-I receptor mediates the prosurvival effect of fibronectin. J Biol Chem 282:26646–26655.

Epa VC, Ward CW. 2006. Model for the complex between the insulin-like growth factor I and its receptor: Towards designing antagonists for the IGF-1 receptor. Protein Eng Des Sel 19:377–384.

French LR, Jackson IT, Melton LJ III. 1990. A population-based study of craniosynostosis. J Clin Epidemiol 43:69–73.

Fulzele K, DiGirolamo DJ, Liu Z, Xu J, Messina JL, Clemens TL. 2007. Disruption of the insulin-like growth factor type 1 receptor in osteoblasts enhances insulin signaling and action. J Biol Chem 282: 25649–25658.

Gabbitas B, Canalis E. 1998. Insulin-like growth factors sustain insulin-like growth factor-binding protein-5 expression in osteoblasts. Am J Physiol 275:E222–228.

Garrett TP, McKern NM, Lou M, Frenkel MJ, Bentley JD, Lovrecz GO, Elleman TC, Cosgrove LJ, Ward CW. 1998. Crystal structure of the first three domains of the type-1 insulin-like growth factor receptor. Nature 394:395–399.

Goode DL, Cooper GM, Schmutz J, Dickson M, Gonzales E, Tsai M, Karra K, Davydov E, Batzoglou S, Myers RM, Sidow A. 2010. Evolutionary constraint facilitates interpretation of genetic variation in resequenced human genomes. Genome Res 20:301–310.

Hirukawa K, Miyazawa K, Maeda H, Kameyama Y, Goto S, Togari A. 2005. Effect of tensile force on the expression of IGF-I and IGF-I receptor in the organ-cultured rat cranial suture. Arch Oral Biol 50: 367–372.

Howard TD, Paznekas WA, Green ED, Chiang LC, Ma N, Ortiz deLuna, Garcia RI, Delgado C, Gonzalez-Ramos M, Kline AD, Jabs EW. 1997. Mutations in TWIST, a basic helix-loop-helix transcription factor, in Saethre–Chotzen syndrome. Nat Genet 15:36–41.

Hu J, McPherson E, Surti U, Hasegawa SL, Gunawardena S, Gollin SM. 2002. Tetrasomy 15q25.3 → qter resulting from an analphoid supernumerary marker chromosome in a patient with multiple anomalies and bilateral Wilms tumors. Am J Med Genet 113:82–88.

Inagaki K, Tiulpakov A, Rubtsov P, Sverdlova P, Peterkova V, Yakar S, Terekhov S, LeRoith D. 2007. A familial insulin-like growth factor-I receptor mutant leads to short stature: Clinical and biochemical characterization. J Clin Endocrinol Metab 92:1542–1548.

Jospe N, Kaplowitz PB, Furlanetto RW. 1996. Homozygous nonsense mutation in the insulin receptor gene of a patient with severe congenital insulin resistance: Leprechaunism and the role of the insulin-like growth factor receptor. Clin Endocrinol (Oxf) 45:229–235.

Kant SG, Kriek M, Walenkamp MJ, Hansson KB, van Rhijn A, Clayton-Smith J, Wit JM, Breuning MH. 2007. Tall stature and duplication of the insulin-like growth factor I receptor gene. Eur J Med Genet 50:1–10.

Krivov GG, Shapovalov MV, Dunbrack RL Jr. 2009. Improved prediction of protein side-chain conformations with SCWRL4. Proteins 77: 778–795.

Kruis T, Klammt J, Galli-Tsinopoulou A, Wallborn T, Schlicke M, Muller E, Kratzsch J, Korner A, Odeh R, Kiess W, Pfaffle R. 2010. Heterozygous mutation within a kinase-conserved motif of the insulin-like growth factor I receptor causes intrauterine and postnatal growth retardation. J Clin Endocrinol Metab 95:1137–1142.

Leppig KA, Werler MM, Cann CI, Cook CA, Holmes LB. 1987. Predictive value of minor anomalies. I. Association with major malformations. J Pediatr 110:531–537.

Ma HW, Lajeunie E, de Parseval N, Munnich A, Renier D, Le Merrer M. 1996. Possible genetic heterogeneity in the Saethre–Chotzen syndrome. Hum Genet 98:228–232.

Meyer JL. 1981. Apert's syndrome: (Acrocephalosyndactylism). J Foot Surg 20:210–213.

Mynarcik DC, Williams PF, Schaffer L, Yu GQ, Whittaker J. 1997. Identification of common ligand binding determinants of the insulin and insulin-like growth factor 1 receptors. Insights into mechanisms of ligand binding. J Biol Chem 272:18650–18655.

Nagai T, Shimokawa O, Harada N, Sakazume S, Ohashi H, Matsumoto N, Obata K, Yoshino A, Murakami N, Murai T, Sakuta R, Niikawa N. 2002. Postnatal overgrowth by 15q-trisomy and intrauterine growth retardation by 15q-monosomy due to familial translocation t(13;15): dosage effect of IGF1R? Am J Med Genet 113:173–177.

Online Mendelian Inheritance in Man, OMIM(TM). McKusick–Nathans Institute of Genetic Medicine, Johns Hopkins University (Baltimore, MD) and National Center for Biotechnology Information, National Library of Medicine (Bethesda, MD), August 9, 2010. World Wide Web URL: http://www.ncbi.nlm.nih.gov/omim/.

Passos-Bueno MR, Serti Eacute AE, Jehee FS, Fanganiello R, Yeh E. 2008. Genetics of craniosynostosis: Genes, syndromes, mutations and genotype–phenotype correlations. Front Oral Biol 12:107–143.

Pedersen C. 1976. Letter: Partial trisomy 15 as a result of an unbalanced 12/15 translocation in a patient with a cloverleaf skull anomaly. Clin Genet 9:378–380.

Renteria ME, Gandhi NS, Vinuesa P, Helmerhorst E, Mancera RL. 2008. A comparative structural bioinformatics analysis of the insulin receptor family ectodomain based on phylogenetic information. PLoS One 3:e3667.

Roth DA, Gold LI, Han VK, McCarthy JG, Sung JJ, Wisoff JH, Longaker MT. 1997. Immunolocalization of transforming growth factor beta 1, beta 2, and beta 3 and insulin-like growth factor I in premature cranial suture fusion. Plast Reconstr Surg 99:300–309.

Samudrala R, Moult J. 1998. An all-atom distance-dependent conditional probability discriminatory function for protein structure prediction. J Mol Biol 275:895–916.

Seto ML, Hing AV, Chang J, Hu M, Kapp-Simon KA, Patel PK, Burton BK, Kane AA, Smyth MD, Hopper R, Ellenbogen RG, Stevenson K, Speltz ML, Cunningham ML. 2007. Isolated sagittal and coronal craniosynostosis associated with TWIST box mutations. Am J Med Genet A 143:678–686.

Shuper A, Merlob P, Grunebaum M, Reisner SH. 1985. The incidence of isolated craniosynostosis in the newborn infant. Am J Dis Child 139:85–86.

Sood S, Eldadah ZA, Krause WL, McIntosh I, Dietz HC. 1996. Mutation in fibrillin-1 and the Marfanoid-craniosynostosis (Shprintzen–Goldberg) syndrome. Nat Genet 12:209–211.

Speltz ML, Kapp-Simon K, Collett B, Keich Y, Gaither R, Cradock MM, Buono L, Cunningham ML. 2007. Neurodevelopment of infants with single-suture craniosynostosis: Presurgery comparisons with case-matched controls. Plast Reconstr Surg 119:1874–1881.

Van Allen MI, Siegel-Bartelt J, Feigenbaum A, Teshima IE. 1992. Craniosynostosis associated with partial duplication of 15q and deletion of 2q. Am J Med Genet 43:688–692.

Van den Enden A, Verschraegen-Spae MR, Van Roy N, Decaluwe W, De Praeter C, Speleman F. 1996. Mosaic tetrasomy 15q25 → qter in a newborn infant with multiple anomalies. Am J Med Genet 63:482–485.

Veenma DC, Eussen HJ, Govaerts LC, de Kort SW, Odink RJ, Wouters CH, Hokken-Koelega AC, de Klein A. 2010. Phenotype–Genotype correlation in a familial IGF1R microdeletion case. J Med Genet 47:492–498.

Wallborn T, Wuller S, Klammt J, Kruis T, Kratzsch J, Schmidt G, Schlicke M, Muller E, van de Leur HS, Kiess W, Pfaffle R. 2010. A heterozygous mutation of the insulin-like growth factor-I receptor causes retention of the nascent protein in the endoplasmic reticulum and results in intrauterine and postnatal growth retardation. J Clin Endocrinol Metab 95:2316–2324.

Whittaker J, Groth AV, Mynarcik DC, Pluzek L, Gadsboll VL, Whittaker LJ. 2001. Alanine scanning mutagenesis of a type 1 insulin-like growth factor receptor ligand binding site. J Biol Chem 276:43980–43986.

Zimmerman IL, Steiner VG, Pond RE. 1991. Preschool Language Scale 3rd edition San Antonio: The Psychological Corporation.

Zollino M, Tiziano F, Di Stefano C, Neri G. 1999. Partial duplication of the long arm of chromosome 15: Confirmation of a causative role in craniosynostosis and definition of a 15q25-qter trisomy syndrome. Am J Med Genet 87:391–394.